

Natural Instability of Free Shear Layers

Z. D. Husain* and A.K.M.F. Hussain†
University of Houston, Houston, Texas

Under controlled small-amplitude excitation, an initially laminar free shear layer experiences maximum growth rate at a Strouhal number St_θ of 0.017 (consistent with theory) and maximum growth at $St_\theta \approx 0.011$, while the natural instability frequency $St_{\theta n}$ (of an unexcited shear layer) is found to have an intermediate value. Investigations in both axisymmetric and plane shear layers in a number of independent facilities reveal that the $St_{\theta n}$ value falls in the range 0.0125–0.0155, depending on the exit boundary-layer fluctuation level and the spanwise radius of curvature. The $St_{\theta n}$ value decreases with increasing jet diameter or exit boundary-layer fluctuation level, but is not a direct function of the exit momentum thickness Reynolds number Re_θ . For a given facility, the instability details are found to be independent of whether the entrainment at the lip is parallel to the stream or orthogonal (due to the addition of an end plate). The streamwise evolutions of the amplitudes at the fundamental frequency and its harmonics and subharmonics are unique functions of the downstream distance nondimensionalized by the exit momentum thickness, but their details remain functions of the flow geometry (i.e., axisymmetric or plane). Based on data from different facilities, the successive stages of the natural instability have been characterized.

Introduction

AN initially laminar free shear layer is known to roll up into periodic structures as a result of shear layer instability and nonlinear saturation. The spatial stability theory for the tanh-velocity profile of a free shear layer predicts that the maximum growth rate of a disturbance occurs at the Strouhal number $St_\theta \approx 0.017$ (Refs. 1 and 2). St_θ is the instability frequency nondimensionalized by the exit momentum thickness θ_e and the freestream velocity U_e . In a controlled excitation study of a shear layer, Freymuth³ verified the theory; i.e., the maximum growth rate of the disturbance occurred at $St_\theta \approx 0.017$. This result also has been verified by Miksad⁴ in a two-stream mixing layer and by Zaman and Hussain⁵ in the near field of a circular jet. These studies showed that the maximum amplification occurs at a lower value of St_θ (i.e., at about 0.011).

In contrast, the natural instability (nondimensional) frequency reported by different investigators^{6–10} varied over a range 0.006–0.016. Recognizing the fact that the shear layer instability will lock onto any dominant ambient disturbance within its unstable band, we became curious about whether the natural instability frequency should be expected to vary from one facility to another depending only on the facility disturbances, or if its variation could be traced to flow characteristics such as the exit Re_θ , peak fluctuation level u'_{pe} , jet diameter D , etc. Also, does the natural instability undergo a unique evolution as a function of the nondimensional downstream distance? Does the presence or absence of an exit plate (i.e., the direction of entrainment at the lip) affect shear layer instability? A number of flow facilities available in the laboratory provided an opportunity to explore the answers to these questions.

Experimental Facilities and Procedures

The characteristic length scales (diameter or slit width) of the different facilities used for this study are listed in Table 1. Influences of the jet diameter and exit fluctuation level on the natural instability frequency were investigated in axisym-

metric jets of four different diameters (7.62, 12.7, 18, and 27 cm). The 7.62-cm jet facility has been described in Ref. 11, and the other flow facility, which accepts 12.7, 18, and 27-cm-diam nozzles, has been described in Ref. 12. The plane jet facility was described in Ref. 13.

All velocity data were obtained by linearized constant temperature hot-wire anemometers (TSI 1050 series). Welded 3.8 μ tungsten wires of about 2-mm length were used at an overheat ratio of 0.4. A special custom-made long-prong probe (TSI-1210C) was used for the documentation of the initial condition and for the instability data acquisition. The special probe was used in order to avoid the probe-induced shear layer tone phenomenon.¹⁴ The probe was inclined to the mean stream direction at an angle of 45 deg and approached the shear layer from the low speed side so that the probe stem did not intersect the shear layer. Further details of the data acquisition and initial condition documentation are discussed in Ref. 12. Spectra of linearized velocity signals were obtained with a Spectrascope SD 335 (500 lines) real-time spectrum analyzer. Each spectrum was an ensemble average of 128 separate realizations.

Probe traverses were performed under software control using an inhouse-designed backlash-free traversing mechanism consisting of two orthogonal linear bearings, which permitted independent x and y movements with a resolution of 0.0254 mm. Probe movements were attained by "Slo-syn" stepping motors via a traverse controller, which could be operated in a local "manual mode" in conjunction with an Apple II microprocessor or remotely under program control by laboratory minicomputer (HP 2100S) interfaced with the Apple II microprocessor.

The boundary-layer data were acquired under automated software control of the probe traverse. The linearized hot-wire voltage was digitized by a 12-bit A/D converter at a sampling rate of 500 Hz (maximum available sampling rate was 204 kHz). A 30-s averaging time (covering 15,000 data samples) was used to obtain the mean and rms values at any (x,y) location in the flow. The flow coordinates and the probe orientation are shown in Fig. 1.

Results and Discussion

The Natural Instability Frequency

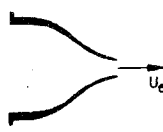
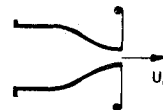


Different flow facilities in the laboratory provided a wide range of flow geometry and exit boundary conditions for studying the natural instability frequency f_n of the free shear

Received May 24, 1982; revision received Nov. 8, 1982. Copyright © American Institute of Aeronautics and Astronautics, Inc., 1983. All rights reserved.

*Professor; presently Senior Research Engineer, Daniel Industries Inc., Houston, Texas. Associate Member AIAA.

†Department of Mechanical Engineering. Associate Fellow AIAA.

Table 1 Instability characteristics of different flow facilities

Diameter, cm	U_e , m/s	$\frac{u'_{ce}}{U_e}$	$\frac{u'_{pe}}{U_e}$	θ_e , mm	f_n , Hz	Re_θ	St_θ	Facility
Axisymmetric free shear layer								
12.7	5	0.0030	0.0040	0.515	148	173	0.0147	
12.7	5	0.0030	0.0035	0.673	104	227	0.0140	
12.7	20	0.0050	0.0093	0.263	1050	354	0.0138	
12.7	20	0.0042	0.0065	0.350	760	476	0.0133	
12.7	45	0.0030	0.0125	0.175	3720	522	0.0145	
12.7	45	0.0028	0.0135	0.196	3150	590	0.0137	
27.0	13	0.0038	0.0060	0.480	360	420	0.0133	
7.62	20	0.0030	0.0330	0.165	1760	222	0.0145	
12.70	20	0.0038	0.0110	0.265	1010	356	0.0134	
Slit-width, cm								
Plane free shear layer								
3.175	5	0.0025	0.0025	0.576	133	194	0.0153	
3.175	20	0.0030	0.0680	0.224	1250	301	0.0140	
45.720	20	0.0040	0.0560	0.182	1420	245	0.0129	
3.175	20	0.0030	0.0380	0.250	1040	336	0.0130	

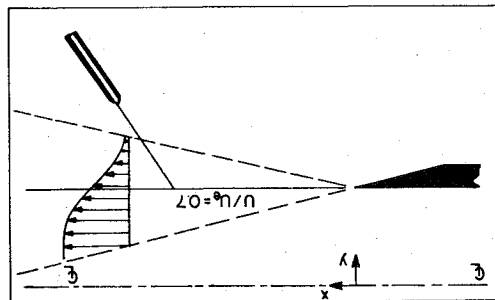
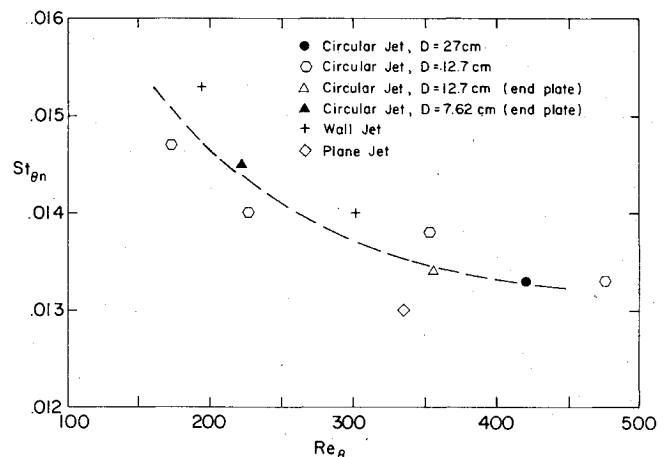


Fig. 1 Flow coordinates and probe orientation.

layer. A preliminary study of the fundamental amplitude profile for the natural instability of free shear layers in a number of flow facilities showed that the peak of the amplitude occurred at the transverse location where $U/U_e = 0.7$ (see also Ref. 3). Since the initiation point and growth rates of different spectral peaks (i.e., at the fundamental and its harmonics and subharmonics) are different, the selection of the sensor location for the determination of the fundamental amplitude is critical. From streamwise evolution of the fundamental, $x/\theta_e \approx 60$ appeared to be the best choice. This location being near the end of the exponential growth of the fundamental (discussed later), the u -spectrum shows a distinct, isolated peak at the fundamental, considerably above the peaks at the harmonics and subharmonics. Thus, $x/\theta_e = 60$ and $U/U_e = 0.7$ was the location chosen for identification of the instability frequency in all facilities and at all speeds reported herein. That is, when the speed was changed in a given facility, the probe was relocated accordingly. By varying the exit speeds in different flow facilities, a wide range of Re_θ was obtained. The nondimensional natural instability frequency St_θ as a function of Re_θ is plotted in Fig. 2, and relevant data are listed in Table 1. The St_θ values for different flow facilities fall in the range 0.0125-0.0155 (Fig. 2). Note that within the data uncertainty, the St_θ value decreases with increasing Re_θ values. For $Re_\theta > 500$, the exit boundary-layer mean velocity profile showed noticeable

Fig. 2 St_θ vs Re_θ data for different flow facilities.

deviation from the Blasius profile, and the peak in the fluctuation level profiles $u'_e(y)$ was high and close to the wall, i.e., the exit boundary layers were disturbed and not laminar.¹² At the exit speed of 20 m/s in the 12.7-cm circular jet, the value of Re_θ was 355 both with and without an end plate. However, the peak u'_{pe} of the exit boundary-layer longitudinal fluctuation intensity profile $u'_e(y)$ for the nozzle with an endplate was higher than that without an endplate, and the corresponding St_θ value was lower. Based on the various initial conditions studied in the different flow facilities, it appears that there is a possible influence of the exit fluctuation level, since a higher Re_θ value for a given flow also implies a higher boundary layer peak fluctuation level u'_{pe}/U_e (Table 1). The u -spectrum under the natural roll-up process shows a hump (Fig. 3), and the uncertainty in θ_e measurement,¹² may have contributed to a relatively large scatter in St_θ values in Fig. 2.

Variations of St_θ

In order to identify possible dependencies of f_n on Re_θ , the jet diameter, and u'_{pe}/U_e level, data were obtained in four

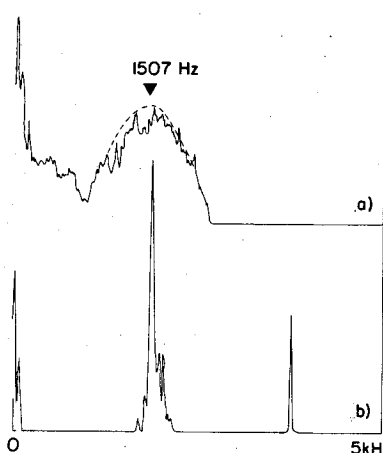


Fig. 3 Effect of feedback excitation on u -spectrum at $x/\theta_e = 60$, $U/U_e = 0.7$ for $U_e = 26.3$ m/s; a) unexcited, b) under feedback excitation. The ordinates are in arbitrary logarithmic (dB) scales.

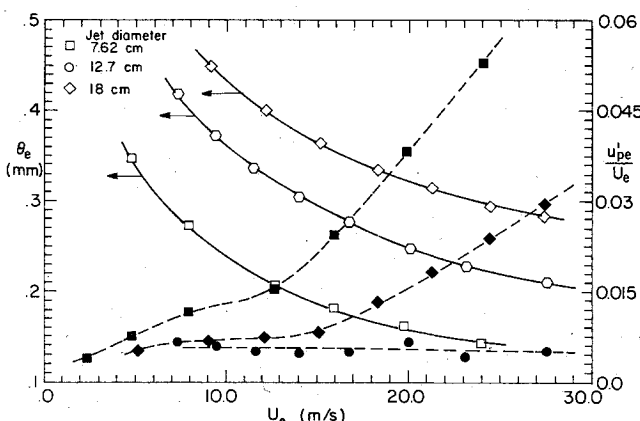


Fig. 4 Variations of exit boundary layer momentum thickness θ_e and peak fluctuation level u'_{pe}/U_e as functions of U_e .

axisymmetric jets (7.62, 12.7, 18, and 27-cm diameters). To minimize the uncertainty in the measurement of θ_e , a number of θ_e values were obtained over the speed range of measurement for each flow facility, and a smooth curve was drawn through plots of θ_e as a function of the exit speed U_e (Fig. 4). The corresponding values of the exit boundary-layer peak longitudinal fluctuation intensity u'_{pe}/U_e are also plotted as a function of U_e . Hence, at any exit speed, the θ_e value and the corresponding Re_θ value were obtained from the curves in Fig. 4. The exit mean velocity profile for the 7.62-cm jet agreed with the Blasius profile, but the exit $u'(y)$ profile showed a noticeable peak for $Re_\theta > 180$ (corresponding to $U_e > 12$ m/s). For the 18-cm jet, the peak in $u'(y)$ profile was above the freestream value when Re_θ was greater than 380 (corresponding to $U_e \approx 15$ m/s).

The exit parameters and instability frequencies for the 7.62- and 18-cm jets are given in Table 2, and the corresponding St_{θ_n} values as functions of the Re_θ value indicate a dependence of St_{θ_n} on u'_{pe}/U_e (Fig. 5). Note that with increasing Re_θ values above 180 and 380 for 7.62- and 18-cm jets, respectively, the St_{θ_n} value decrease continually. In these ranges, the peak fluctuation levels also increase with Re_θ . The decrease in the St_{θ_n} value is noticeably rapid with increasing Re_θ values. Note also that with the Re_θ value being nearly proportional to $U_e^{1/2}$, the speed range is quite large for a small Re_θ range (Fig. 5).

The Azimuthal Curvature Effect

The St_{θ_n} value is essentially constant for a given flow facility when the exit fluctuation intensity profile does not

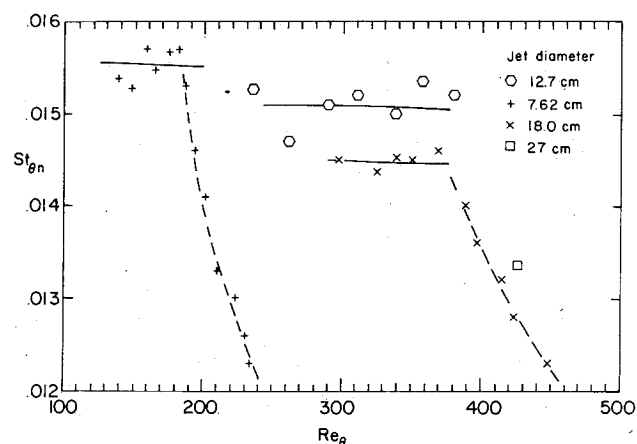


Fig. 5 St_{θ_n} vs Re_θ relationship for different diameter jets.

Table 2 Exit parameters and instability frequency

U_e , m/s	θ_e , mm	f_n , Hz	Re_θ	St_θ
a) 7.62-cm circular jet (unexcited)				
23.3	0.149	1920	234	0.0123
21.9	0.156	1770	230	0.0126
20.6	0.161	1670	223	0.0130
18.9	0.165	1530	210	0.0133
16.9	0.177	1350	201	0.0141
15.5	0.185	1220	193	0.0146
14.0	0.197	1090	186	0.0153
12.8	0.210	960	181	0.0157
11.7	0.221	830	174	0.0157
10.5	0.232	700	164	0.0155
9.6	0.245	615	158	0.0157
8.3	0.264	480	147	0.0153
7.2	0.284	390	138	0.0154
b) 18-cm circular jet (unexcited)				
21.1	0.315	826	447	0.0123
19.3	0.326	760	423	0.0128
18.2	0.338	712	414	0.0132
17.1	0.345	676	397	0.0136
16.2	0.356	636	388	0.0140
14.8	0.370	586	368	0.0146
13.6	0.382	516	350	0.0145
12.7	0.396	466	338	0.0145
11.8	0.408	416	324	0.0144
10.1	0.437	336	297	0.0145

have any noticeable peak. The natural instability frequency of a 27 cm jet was found to be at $St_{\theta_n} \approx 0.0133$ for $Re_\theta = 420$. Thus, if only the initial conditions with low boundary-layer disturbance levels are considered, the natural instability frequency corresponds to the St_{θ_n} values of about 0.0156, 0.0151, 0.0145, and 0.0133 for diameters 7.62, 12.7, 18, and 27 cm, respectively (Fig. 5). These data suggest that the natural instability frequency is also a function of the jet diameter and that the St_{θ_n} value decreases with increasing jet diameter. The plane shear layer (with infinite radius) value of $St_{\theta_n} \approx 0.012$ is also consistent with this trend. Michalke¹⁵ took into account the azimuthal curvature effect in his theoretical analysis of a laminar, inviscid, parallel shear layer. This theory also predicts that the St_θ value corresponding to the most unstable mode decreases with increasing D/θ_e , consistent with the present experimental observations.

Dependence on Re_θ and u'_{pe}/U_e

The experimental values of St_{θ_n} were found to progressively decrease with increasing values of u'_{pe}/U_e . However, since there is a corresponding increase in the Re_θ value, it was considered worthwhile to separate the effects of u'_{pe}/U_e and Re_θ . For this purpose, the shear layer of the 12.7-cm jet was

Table 3 Instability frequency of 12.7-cm jet (under excitation)

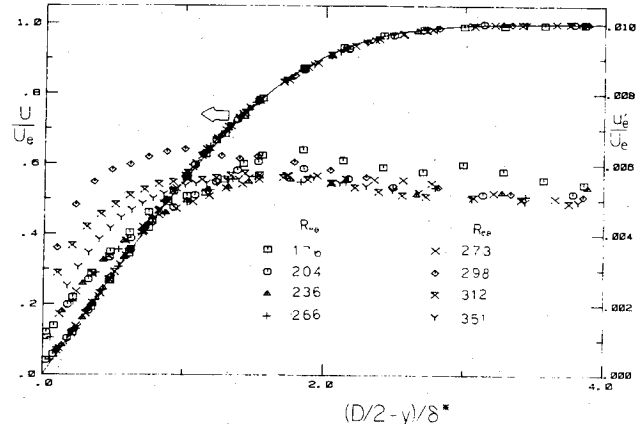
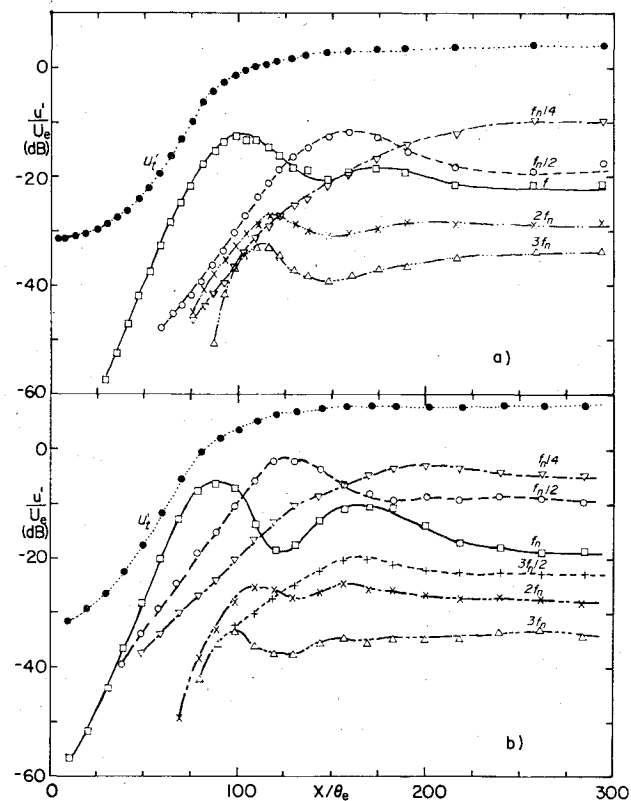
U_e , m/s	θ_e , mm	f_n , Hz	Re_θ	St_θ
9.4	0.372	386	235	0.0153
11.4	0.340	492	261	0.0147
14.2	0.304	704	290	0.0151
16.7	0.278	912	311	0.0152
20.1	0.250	1208	338	0.0150
23.3	0.228	1507	357	0.0154
26.3	0.214	1870	380	0.0152

investigated. The exit boundary layer shows identical mean profiles (agreeing with the Blasius profile) for a number of exit speeds with no noticeable peak in the $u'_e(y)$ profile (Figs. 4 and 6). Since u'_{pe} was held constant while Re_θ varied over a range, this experiment would establish any direct dependence of $St_{\theta n}$ on Re_θ . To enhance the roll-up phenomenon, the velocity signal from a reference probe placed at $x/\theta_e = 60$ and $U/U_e = 0.85$ was used directly (without filtering) to drive the speaker attached to the jet settling chamber; the excitation of the settling chamber as a cavity was maintained at a very low level, such that the exit centerline value of u'_e was increased by 0.01% of U_e over the unexcited condition. Remember that f_n was identified from the u -spectrum, obtained from the velocity signal of the traversing probe located at $x/\theta_e = 60$ and $U/U_e = 0.7$. As expected, this feedback excitation technique introduced a noticeable change in the spectral content of the velocity signal (Fig. 3). Since this feedback excitation organized the initial shear layer roll-up and reduced the phase jitter of the natural case, a clear peak appeared at f_n . This reduced the uncertainty in the determination of f_n and the corresponding value of $St_{\theta n}$. The position of this reference probe in x has a weak influence on the f_n value under this feedback excitation technique, but the variations in the f_n value for the probe location varying within $\pm 5\theta_e$ around $x/\theta_e = 60$ was less than the data uncertainty. It is interesting to note that even though Re_θ was varied between 235 and 380, the $St_{\theta n}$ value remained constant at about 0.0151 (Table 3). This, therefore, shows that $St_{\theta n}$ is not a direct function of Re_θ but a strong function of u'_{pe}/U_e , its value decreasing with increasing values of u'_{pe}/U_e . It is worth noting that the time-average measures of the shear layer for a given u'_{pe}/U_e were reported to be independent of Re_θ .¹⁶

The reasons for the dependence of $St_{\theta n}$ directly on u'_{pe}/U_e are not totally clear. One plausible explanation is proposed here. It has been found that with increasing u'_{pe}/U_e , the relaxation of the exit (Blasius) mean velocity profile to the free shear layer (i.e., tanh-type) profile occurs earlier in x .¹² Theoretical analysis of Ref. 2 has shown that the most unstable frequency $St_{\theta n}$ is a strong function of the profile shape. The $St_{\theta n}$ value decreases monotonically from the Blasius profile to the tanh profile. The theoretical analysis is, therefore, consistent with the dependence of $St_{\theta n}$ on u'_{pe}/U_e experimentally observed here.

The Evolution Stages of Natural Instability

In an attempt to characterize the evolution of the natural instability, the streamwise variations of the amplitudes at f_n and its harmonics and subharmonics were documented for different initial conditions in both plane and axisymmetric free shear layers over $0 \leq x/\theta_e \leq 300$. The evolution of the amplitude at f_n and its harmonics and subharmonics were obtained from the u -spectra along the $U/U_e = 0.7$ line. Plots of the amplitudes of different frequencies as functions of the downstream distance for plane and axisymmetric free shear layers showed a definite evolution pattern; Fig. 7 shows the plot for an exit speed of 5 m/s. Similar evolution patterns were observed at other speeds for both plane and axisymmetric free shear layers. The downstream distance x , normalized by the exit momentum thickness θ_e , showed a collapse of data for plane as well as axisymmetric mixing layers.

**Fig. 6** Exit boundary layer $U(y)$ and $u'(y)$ profiles at different Re_θ ; $D=12.7$ cm.**Fig. 7** Streamwise evolutions of amplitudes at the fundamental (f_n) and its harmonics and subharmonics at $U_e = 5$ m/s; a) axisymmetric shear layer for $D = 12.7$ cm; b) plane shear layer of 3.175 cm slit plane jet.

Amplitudes at f_n and $f_n/2$ for both plane and axisymmetric mixing layers are plotted in Fig. 8, which shows agreement among data in different facilities. An average line drawn through data at each frequency shows the evolution of the amplitude at the fundamental and its harmonics and subharmonics. Figure 9 shows these average lines for the fundamental, harmonics, and subharmonics.

Even though there are some differences in the details of the amplitude evolution patterns for the axisymmetric (Fig. 9a) and plane (Fig. 9b) shear layers, the progressions of the transition process are very similar. On the basis of the similar features, the progression of the natural instability is divided into eight characteristic streamwise spatial regions shown in Figs. 9a and b.

Region I: In this region, the u -spectrum has a peak at f_n and none at the harmonics and subharmonics because these

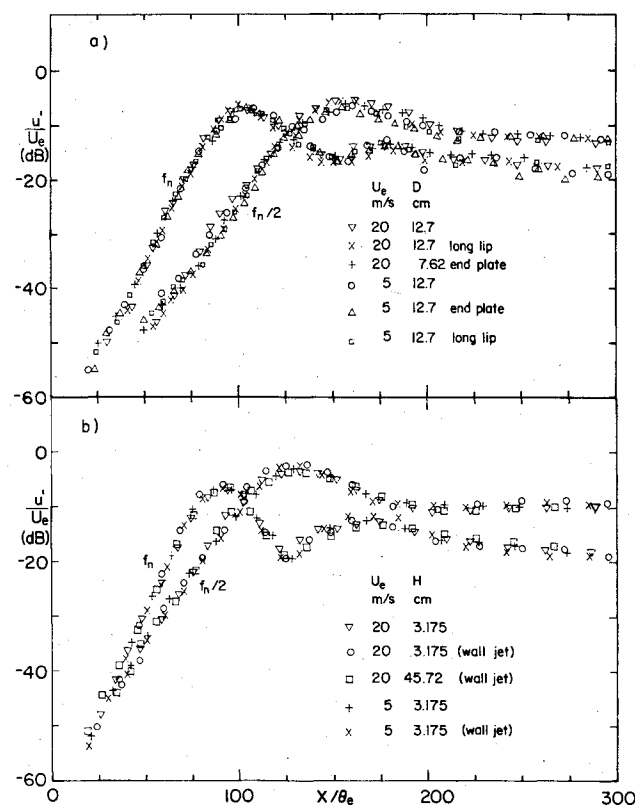


Fig. 8 Streamwise evolutions of f_n and $f_n/2$ amplitudes for different facilities and speeds; a) axisymmetric shear layer, b) plane shear layer.

are at the noise level. The amplitude at f_n shows an exponential growth in x over this region.

Region II: The amplitude at f_n continues to grow exponentially, and a subharmonic peak appears in the u -spectrum. Note that regions I and II occur at relatively smaller x/θ_0 in the plane shear layer than in the axisymmetric shear layer. The exit fluctuation level for plane shear layers was higher than those in axisymmetric cases (Table 1). Data in the plane shear layer show a relatively higher growth rate of the fundamental, which may be due to the differences in the geometry.

Region III: The beginning of this region is marked by the saturation of the fundamental amplitude. Amplitudes at f_n and $f_n/2$ continue to grow exponentially and indicate the evolution of the pairing process. The nonlinear saturation at f_n results in peaks at higher harmonics; consequently, amplitudes at f_n and $f_n/2$ also grow in x . Note that a peak at $3f_n/2$ is observed for the plane shear layer only. Although none of the axisymmetric cases showed peaks at $3f_n/2$ for the natural instability, Zaman and Hussain⁵ reported peaks at $3f_n/2$ in an axisymmetric shear layer under controlled excitation. Note that the axisymmetric layers show lower amplitudes at all frequencies of interest in comparison with those in plane layers (Fig. 7). The absence of the $3f_n/2$ component in the axisymmetric layer is perhaps due to the lower amplitudes of the fundamental (f_n) and the subharmonic ($f_n/2$).

Region IV: The amplitude at f_n decreases while the amplitudes at $f_n/2$ and $f_n/4$ continue to grow exponentially, indicating that the first pairing stage occurs over this region. Amplitudes of higher harmonics equilibrate.

Region V: This region marks the saturation of $f_n/2$ and continued exponential growth at $f_n/4$, indicating the beginning of the second stage of pairing. The fundamental and higher harmonics show local maxima in their respective amplitudes.

Region VI: In this region, the fundamental reaches a second peak value; the evolution of the $f_n/4$ component becomes nonlinear, indicating strong activity associated with

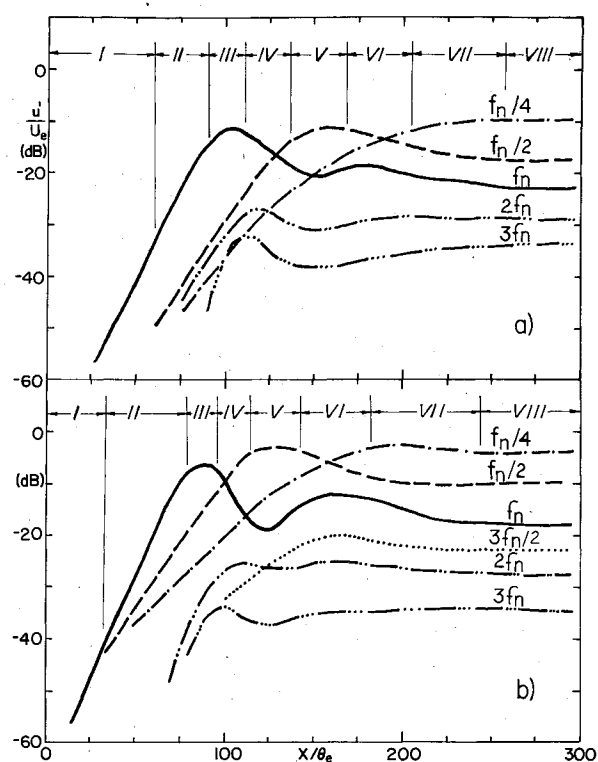


Fig. 9 Characteristic transition stages; a) axisymmetric shear layer, b) plane shear layer.

the second state of pairing and a concomitant decrease in the subharmonic amplitude.

Region VII: Equilibration of the second subharmonic amplitude; both f_n and $f_n/2$ components decrease in amplitude. The spectrum begins to become broadband.

Region VIII: This region marks the achievement of complete spectral broadening, the higher harmonic peaks in the spectrum being lost in the broadband turbulence. The time-average measures show self-preservation starting at this location.^{12,17}

The streamwise evolution of the amplitudes of different frequencies in an excited two-stream shear layer was reported by Miksad⁴ in the laboratory coordinates for only one flow condition. Since the initial fundamental amplitude was higher in the excited case, regions I and II were relatively short, due to earlier saturation. However, regions III, IV, and V were farther downstream when compared with the natural instability case reported here. This is to be expected, because the velocity of propagation of the disturbance is higher due to advection in the two-stream shear layer, and thus the spatial growth should be slower.

Concluding Remarks

The most unstable St_θ for a free shear layer was theoretically predicted to be 0.017, and has been experimentally verified in different studies via controlled excitations of axisymmetric and plane shear layers. These experiments also revealed that the maximum amplification occurs at a much lower St_θ (about 0.011) and has a longer evolution distance at this lower frequency. The observation that a free shear layer in the absence of any controlled excitation naturally rolled up at an $St_{\theta n}$ value intermediate to these two values prompted the investigation of the natural instability frequency in a number of flow facilities. This paper summarizes these $St_{\theta n}$ data and documents the dependence of $St_{\theta n}$ on the freestream velocity, exit fluctuation level, flow geometry (i.e., plane and axisymmetric layers), jet diameter, and exit entrainment direction. It also identifies the different

characteristic stages in the progression of the transition in unexcited shear layers. Care was taken to orient the custom-made, long-pronged hot wire probe to avoid the probe-induced shear layer tone.

The natural instability frequency $St_{\theta n}$ has been found to fall within the range 0.0128-0.0155, depending on the jet diameter and exit boundary-layer peak fluctuation level u'_{pe}/U_e . For a given exit fluctuation level u'_{pe}/U_e , the $St_{\theta n}$ value decreases with increasing jet diameter, consistent with theoretical predictions. For a given facility, $St_{\theta n}$ decreased monotonically with increasing Re_θ . Since increasing Re_θ in general implies progressively increasing values of u'_{pe}/U_e , it was felt necessary to separate the effects of Re_θ and u'_{pe}/U_e . For a facility where u'_{pe}/U_e remained constant, it is shown that $St_{\theta n}$ remained unchanged while Re_θ was varied. This conclusively established that $St_{\theta n}$ depends on u'_{pe}/U_e and decreases with increasing values of u'_{pe}/U_e . A plausible explanation for this has been presented in terms of the enhanced spreading of the shear layer with increasing u'_{pe}/U_e .

The instability characteristics of the shear layer have been found to be independent of whether the entrainment at the lip is parallel or orthogonal to the main stream (due to the absence or presence of an end plate).

Experiments revealed that there are noticeable differences between the instability details of axisymmetric and plane shear layers. These differences are perhaps attributable to the influence of the spanwise curvature of the shear layer.

In spite of the differences between the instability characteristics of axisymmetric and plane layers, the streamwise evolutions of the amplitudes of the fundamental and its harmonics and subharmonics show strong similarities. On the basis of these, eight characteristic stages in the streamwise evolution of the natural instability have been identified. The spectral evolution is complete at $x/\theta_e \cong 300$, which was also found to be the beginning of self-preservation of the layer.

Acknowledgments

This research was funded by the NASA Ames Research Center Grant NSG-2337 and the National Science Foundation Grant MEA-811676.

References

- ¹Michalke, A., "On Spatially Growing Disturbances in an Inviscid Shear Layer," *Journal of Fluid Mechanics*, Vol. 23, 1965, pp. 521-544.
- ²Michalke, A., "The Instability of Free Shear Layers," *Progress in Aero Science*, Vol. 12, 1972, pp. 213-239.
- ³Freymuth, P., "On Transition in a Separated Laminar Boundary Layer," *Journal of Fluid Mechanics*, Vol. 25, 1966, pp. 683-704.
- ⁴Miksad, R. W., "Experiments on Non-linear Stages of Free Shear Layer Transition," *Journal of Fluid Mechanics*, Vol. 56, 1972, pp. 695-719.
- ⁵Zaman, K.B.M.Q. and Hussain, A.K.M.F., "Vortex Pairing in a Circular Jet Under Controlled Excitation. Part I. General Jet Responses," *Journal of Fluid Mechanics*, Vol. 101, 1980, pp. 449-491.
- ⁶Sato, H., "Experimental Investigation on the Transition of Laminar Separated Layers," *Journal of the Physical Society of Japan*, Vol. 11, 1956, pp. 702-709.
- ⁷Sato, H., "Further Investigation on the Transition of Two-dimensional Separated Layers at Subsonic Speeds," *Journal of the Physical Society of Japan*, Vol. 14, 1959, p. 1797-1810.
- ⁸Michalke, A. and Wille, R., "Strömungsvorgänge in laminar-turbulenten Übergangsbereich von Freistrahlgrenzschichten," *Applied Mechanics Proceedings*, edited by H. Görtler, 11th International Congress of Applied Mechanics, Springer, Munich, 1966, pp. 962-972.
- ⁹Pfizenmaier, E., "Zur Instabilität des Schallbeeinflussten Freistrahls," Doktor-Ingenieur Thesis, Technische Universität, Berlin, 1973.
- ¹⁰Davies, P.O.A.L. and Baxter, D.R.J., "Transitions in Free Shear Layers," *Lecture Notes in Physics*, edited by H. Fiedler, Vol. 73, 1978, pp. 125-135.
- ¹¹Zaman, K.B.M.Q., "An Experimental Investigation of Vortex Pairing in a Circular Jet Under Controlled Excitation," Ph.D. Dissertation, Univ. of Houston, 1978.
- ¹²Husain, Z. D., "An Experimental Study of Effects of Initial and Boundary Conditions on Near and Far Fields of Jet Flows," Ph.D. Dissertation, Univ. of Houston, 1982.
- ¹³Hussain, A.K.M.F. and Clark, A. R., "Upstream Influence on the Near Field of a Plane Turbulent Jet," *The Physics of Fluids*, Vol. 20, 1977, pp. 1416-1426.
- ¹⁴Hussain, A.K.M.F. and Zaman, K.B.M.Q., "The Free Shear Layer Tone Phenomenon and Probe Interference," *Journal of Fluid Mechanics*, Vol. 87, 1978, pp. 349-383.
- ¹⁵Michalke, A., "Instabilität eines kompressiblen runden Freistrahls unter Berücksichtigung des Einflusses der Strahlgrenzschichtdicke," *Zeitschrift Für Flugwissenschaften*, Vol. 19, July 1971, pp. 319-328.
- ¹⁶Hussain, A.K.M.F. and Zedan, M. F., "Effects of the Initial Condition on the Axisymmetric Free Shear Layer: Effects of the Initial Momentum Thickness," *The Physics of Fluids*, Vol. 21, 1978, pp. 1100-1112.
- ¹⁷Husain, Z. D. and Hussain, A.K.M.F., "Axisymmetric Mixing Layer: Influence of the Initial and Boundary Conditions," *AIAA Journal*, Vol. 17, Jan. 1979, pp. 48-55.